Tropical forest carbon assessment: integrating satellite and airborne mapping approaches

Gregory P Asner

Department of Global Ecology, Carnegie Institution for Science, 260 Panama Street, Stanford,
CA 94305, USA

E-mail: gpa@stanford.edu

Abstract
Large-scale carbon mapping is needed to support the UNFCCC program to reduce deforestation
and forest degradation (REDD). Managers of forested land can potentially increase their carbon
credits via detailed monitoring of forest cover, loss and gain (hectares), and periodic estimates
of changes in forest carbon density (tons ha^{-1}). Satellites provide an opportunity to monitor
changes in forest carbon caused by deforestation and degradation, but only after initial carbon
densities have been assessed. New airborne approaches, especially light detection and ranging
(LiDAR), provide a means to estimate forest carbon density over large areas, which greatly
assists in the development of practical baselines. Here I present an integrated satellite–airborne
mapping approach that supports high-resolution carbon stock assessment and monitoring in
tropical forest regions. The approach yields a spatially resolved, regional state-of-the-forest
carbon baseline, followed by high-resolution monitoring of forest cover and disturbance to
estimate carbon emissions. Rapid advances and decreasing costs in the satellite and airborne
mapping sectors are already making high-resolution carbon stock and emissions assessments
viable anywhere in the world.

Keywords: biomass mapping, carbon accounting, deforestation, forest degradation, LiDAR,
REDD, satellite mapping, UNFCCC

1. Introduction

The United Nations Framework Convention on Climate
Change (UNFCCC) is facilitating large-scale forest monitoring
for Reduced Deforestation and Degradation (REDD; http://
unfccc.int/methods_science/redd/items/4531.php). In support
of REDD, the Intergovernmental Panel on Climate Change
(IPCC 2006) provided guidelines to assist countries in
developing carbon assessment methodologies. These
guidelines are organized into three 'Tiers', each providing
successively increased accuracy and thus potentially higher
financial returns for monitoring and verifying carbon stocks
and emissions. The Tier I approach is the most general,
based on simple nationwide estimates of forest cover and
generic forest carbon density values (e.g., tons of carbon per
hectare). Tiers II and III provide increased detail on carbon
stocks and emissions at regional and national levels using a
combination of plot inventory, satellite mapping and carbon
modeling approaches. To achieve Tier III levels of accuracy,
both aboveground and belowground live and dead carbon
stocks must be estimated and modeled (Gibbs *et al* 2007).

At the national scale, many tropical countries will rely
initially on Tier I levels of accuracy based on average
biomass and soil carbon values assigned for biomes and large
geographic regions, which will generate large uncertainties
and thus potentially lower carbon credits (Gibbs *et al* 2007,
Angelson *et al* 2009). Conservative accounting guidelines
from the IPCC require that users of Tier I estimates assign a
relatively low carbon stock per hectare compared to what might
be achieved if more detailed measurements are conducted.

Developing regional and national monitoring capacities above Tier I accuracies will require improved high-resolution carbon mapping and modeling approaches, with the pay-off realized as increased carbon credit, boosted carbon sequestration, and improved ecosystem protection.

Gibbs *et al* (2007) point out that, in tropical forests, the majority of carbon is sequestered in aboveground live tissues (e.g. trees), with secondary stocks in soils and coarse woody debris. Root and soil carbon stocks average about 20% of total carbon stored in tropical forests (Cairns *et al* 1997), and the necromass produced by tree mortality averages ∼10% of aboveground live biomass (Brown *et al* 1995, Keller *et al* 2004). One major exception rests in the large belowground carbon stocks found in peat swamps of SE Asia. Notwithstanding peats, the major unknown rests in the aboveground live biomass, and thus it is my focus here.

To monitor aboveground carbon stocks, including carbon losses and gains caused by deforestation, forest degradation and forest recovery, a combination of data is required: (i) the rate of change in forest cover and disturbance; and (ii) the amount of carbon stored in the forest ('carbon density' in units such as tons of carbon per hectare: tons $C \, ha^{-1}$). Various satellites measure forest cover, canopy loss and disturbance, and metrics of forest structure (Chambers *et al* 2007), but no satellite technology can directly measure carbon density (GOFC-GOLD 2009). Satellites thus provide an opportunity to monitor changes in forest carbon caused by deforestation and degradation but only if carbon densities have been assessed. Traditionally, carbon densities have been assessed using field-based inventory plots, which are valuable but also expensive, time consuming and inherently limited in geographic representativeness. A survey of the major plots networks in Amazonia suggests that less than one-millionth of the region has been measured in the field, albeit in an effort to be statistically representative (synthesized by Phillips *et al* 1998, Saatchi *et al* 2007). However, the natural variation in forest structure and biomass, combined with the enormous geographic extent and rate of forest loss and disturbance, makes field plots difficult to use (alone) for assessing tropical forest carbon densities over large areas. Such field-based monitoring would require thousands of plots and regular revisits using laborious hand measurement techniques. New approaches are needed to extend field plot networks, and to bridge a gap between field measurements and satellite observations.

Airborne mapping methods may assist in developing carbon stock estimates in tropical forests (Brown *et al* 2005). The latest airborne approaches, especially light detection and ranging (LiDAR), can be used to estimate aboveground carbon stocks over large areas (reviewed by Lefsky *et al* 2002b). LiDAR mapping, when combined with field calibration plots, can yield aboveground carbon maps over thousands of hectares per day of flying. Here I propose that LiDAR-based maps can be used in a baseline analysis to initiate a long-term monitoring program that will subsequently rely primarily on low-cost satellite data and analysis methods. However, given the limited work attempting to integrate airborne technologies into the carbon mapping process for REDD,

there are no operational or even any clearly proposed methods for using these technologies. How would the new airborne LiDAR mapping approaches be used with satellite and plot measurement methods to estimate aboveground carbon stocks? And what satellite monitoring technology is available today to support such a monitoring approach? This paper presents a conceptual framework for integrating new satellite monitoring technology with infrequent aircraft-based mapping, and a modest number of field plots, to set baselines and to monitor carbon stocks, losses and recovery in forests at the sub-national level. The primary focus here is on tropical forests, but many of the concepts presented are readily transferable to other forest types.

2. Overview of technical approach

An approach to support Tier II/III carbon stock estimation involves two tasks: develop a spatially resolved, regional state-of-the-forest carbon baseline; and monitor forest cover change to estimate losses or gains in forest carbon stocks. The first task can be described in four detailed steps: (a) satellite analysis of forest cover and condition; (b) stratified sampling of forest canopy three-dimensional (3D) structure using airborne LiDAR; (c) conversion of LiDAR structural data to aboveground carbon density estimates using new LiDAR allometrics along with a limited number of field plots; and (d) integration of the satellite map with the airborne LiDAR data to set a regional, high-resolution baseline carbon stock estimate. The second major task involves long-term monitoring of carbon losses and gains using satellite data and models. This task involves at least three steps: (i) continuous monitoring of forest cover losses and gains using satellite imagery; (ii) conversion of mapped losses in forest cover and degradation to carbon emissions; and (iii) modeling of carbon gains in intact forest and secondary regrowth. These major tasks, and the steps required to achieve them, are discussed and illustrated in the following sections. The last step, on modeling carbon gains, is only partially covered here, since modeling of carbon accumulation is demonstrated and synthesized elsewhere (e.g., Hirsch *et al* 2004, IPCC 2006).

3. State-of-the-forest carbon baseline

There is much debate in the REDD monitoring arena regarding the development of baseline carbon assessments (reviewed by Olander *et al* 2008). This debate is largely political, with most parties focusing on the time period in which to set the baseline carbon stock. Nonetheless, forest management or conservation organizations will need to create a current baseline of forest carbon stocks, from which to monitor change into the future. Since no satellites can directly measure forest carbon, a baseline assessment must be developed using a combination of maps that include regional forest cover and condition, plus estimates of forest carbon densities. An illustrated flow diagram depicting the outputs of each step is shown in figure 1, with each step noted in the diagram.
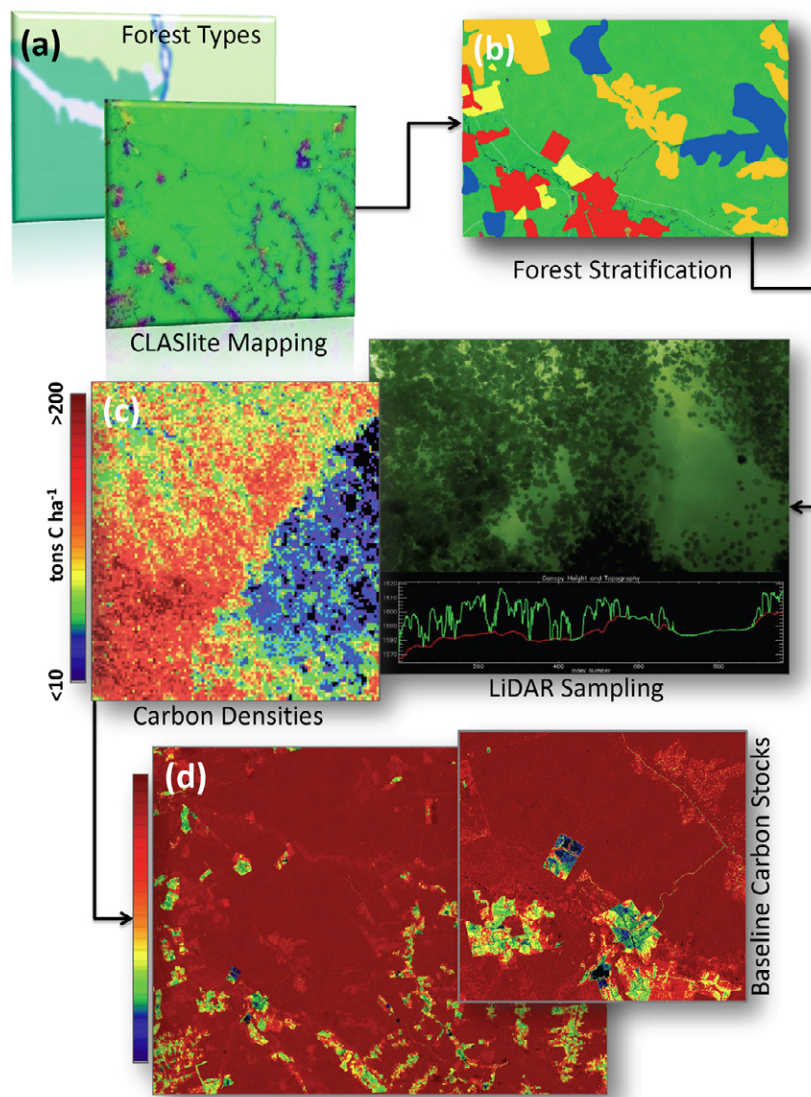
Figure 1. Illustrated flow diagram depicting an approach to: (a) assess forest cover and disturbance with satellite imagery, (b) stratify the forested landscape, (c) sample the carbon densities of each major forest type using airborne light detection and ranging (LiDAR), and (d) estimate the baseline carbon stocks throughout the region of interest.

3.1. Mapping forest type, cover and condition

A first step to developing a spatially-detailed forest carbon assessment involves the acquisition and/or development of a map depicting forest type, deforestation and disturbance (figure 1(a)). In recent years, many maps have become available showing forest type at national and sub-national levels. These maps typically provide categories such as 'terra firme', 'bamboo-dominated', 'open woodland', and others considered appropriate to the region of interest and to the map scale. Some of these maps are derived from satellite data, whereas many are created from a combination of aerial photography and field surveys. A map of forest type will aid in partitioning the landscape into categories for subsequent airborne and field measurements, as described later. The more detailed the map, the more finely the landscape can be partitioned for biomass sampling.

Although laborious to create, maps of forest type rarely require complete redevelopment unless a major shift in forest cover occurs. Most maps of forest type are available from regional and national government sources, non-government organizations or international sources such as the World Conservation Monitoring Centre of the United Nations (http://www.unep-wcmc.org/forest/global_map.htm) and the European Commission's Global Land Cover 2000 (http://bioval.jrc.ec.europa.eu/products/glc2000/products.php). An example map developed by the Brazilian government is shown in figure 2.

Maps of deforestation and disturbance are more difficult to obtain, but are essential to developing an initial regional carbon stock estimate. Various satellite techniques are available with spatial resolutions of <10 to 1000 m or more (reviewed by DeFries *et al* 2005, Achard *et al* 2007, GOFC-GOLD 2009). For regional to national level mapping of forest cover, it is advantageous to use moderate-resolution satellites such as Landsat (30 m) and SPOT (10–20 m) because these systems resolve forest clearings down to about
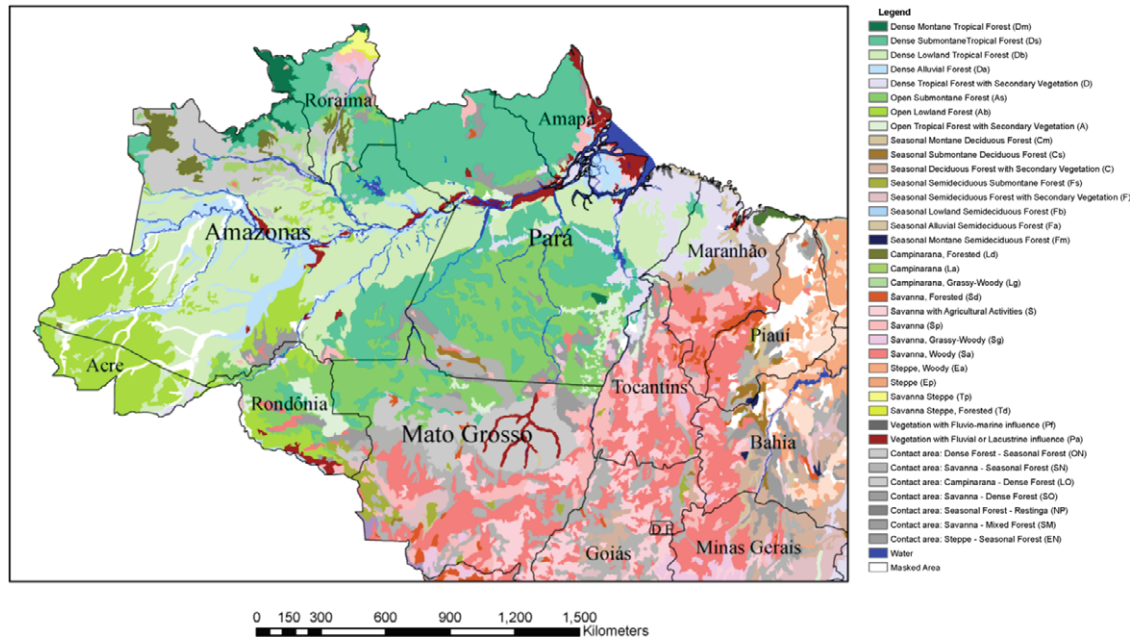
Figure 2. Example map of forest and other ecosystem types in the Brazilian Legal Amazon (IBGE 1993).

0.1 ha resolution. Moreover, newer analytical approaches use the same moderate-resolution imagery to resolve much finer forest disturbances caused by selective logging, small-scale clearing and other land-use processes (Souza *et al* 2005). The Carnegie Landsat Analysis System (CLAS) is one such system, developed to map forest disturbances such as selective logging (Asner *et al* 2005, 2006). Recently, CLASlite was created to provide automated mapping of forest cover, deforestation and disturbance using a wide range of satellite sensors (http://claslite.ciw.edu). CLASlite is easy to use, well tested on standard desktop computers, free of charge, and it is currently being disseminated to government and non-government agencies in South America. CLASlite can be used with a variety of freely available satellite imagery, such as Landsat, ASTER or MODIS, or with commercial SPOT imagery. For example, Landsat 5 and 7 imagery is now completely free of charge from the United States Geological Survey (http://landsat.usgs.gov) and from the Brazilian National Institute for Space Research (http://www.dgi.inpe.br). This is further discussed in the subsequent section on costs.

Typical image results from the CLASlite step are shown using Landsat 7 imagery over an 8000 km^2 sample area in the eastern Brazilian Amazon (figure 3). This analysis was fully automated, taking 20 min on a standard desktop computer and with no technical training (described in detail by Asner *et al* 2009b). Forest cover, deforested areas, and forest disturbance—here, caused primarily by selective logging—are readily observed in the CLASlite imagery. It is important to note that each CLASlite image pixel reports a percentage of forest canopy, dead vegetation and bare soil (0–100% for each of these surface types). These percentages precisely indicate the amount of forest damage per pixel (Asner *et al* 2004). This is critical to delineating areas of wholesale clearing (>80%

forest cover loss in a pixel) versus forest degradation associated with the partial clearing of a pixel.

3.2. Forest stratification and airborne LiDAR sampling

Using the maps derived from CLASlite combined with maps of forest type, the region can be stratified into LiDAR mapping units (figure 1(b)). These mapping units will vary in size and regional importance, providing the user with an opportunity to prioritize them based on a variety of criteria such as potential biomass, biodiversity hotspots, risk of deforestation or degradation, and other factors. The prioritization of LiDAR mapping units will be highly dependent upon the specific interests and needs of the user. For carbon assessment purposes, the map could be prioritized to cover areas of intact forest likely harboring the highest biomass as well as areas of recent selective logging or secondary regrowth that will undergo carbon accumulation in the years following the baseline assessment (figure 4).

Airborne LiDAR mapping involves flight planning, sensor calibration, data acquisition, post-flight image calibration, and 3D data generation phases (reviewed by Lefsky *et al* 2002b). There is a rapidly growing industry for commercial LiDAR mapping available throughout the world that can accommodate these tasks. In fact, one market analysis reports that, between 2005 and 2008, there was a 75% increase in the number of airborne LiDAR systems and a 53% increase in the volume of LiDAR operators worldwide (http://www.caryandassociates.com/marketing_tools/market_reports/rpt4.html). As a result, LiDAR operators can provide data acquisition services nearly anywhere in the world today. Research and demonstration systems, such as the Carnegie Airborne Observatory (CAO; http://cao.ciw.edu), integrate LiDAR with other imaging sensors to facilitate mapping of both forest composition and 3D structure simultaneously (Asner *et al* 2007). Independent
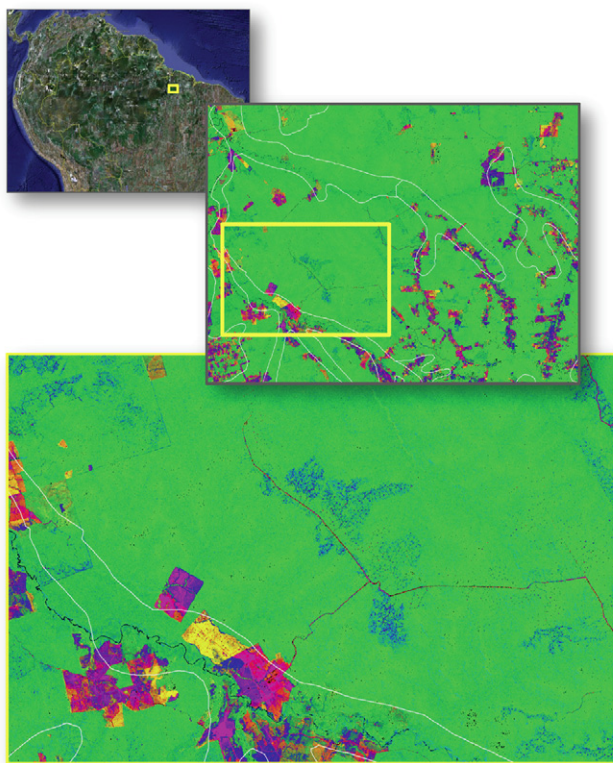
Figure 3. Example CLASlite image results for an 8000 km² region of the eastern Brazilian Amazon. Top panel shows location of this area in South America; middle panel shows the entire region; bottom panel shows a 1500 km² zoom image. CLASlite imagery provides a percentage (0–100%) canopy cover of live/forest vegetation, dead or senescent vegetation, and bare soils. Recently deforested and/or burned areas are obvious with high bare soil fractions (reds, magenta); forest regrowth is apparent as large fractions of green canopy intertwined with exposed soils (yellows); selectively logged forest (blue patterns in forest); and intact forest (nearly solid green).
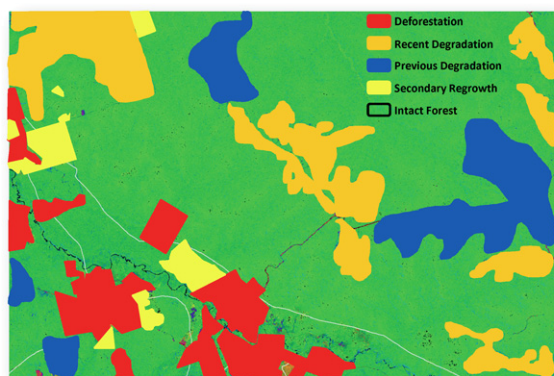

Figure 4. Stratification of the forested region using vegetation map from figure 2 and CLASlite output from figure 3. White lines indicate the general delineation between upland (terra firme) and low-lying/drainage areas.

of whether the source is commercial, government or research, airborne LiDAR provides an opportunity to map the 3D structure of forest canopies over more than 5000 ha per day at 1.0 m spatial resolution.
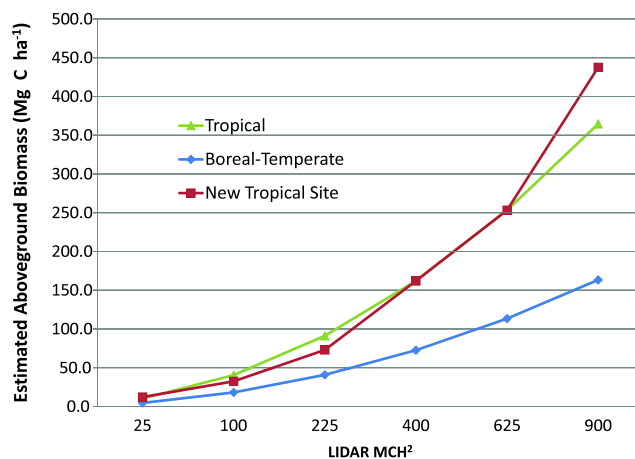

Figure 5. Example relationships between airborne LiDAR measurements of mean canopy vertical height profiles (MCH) and field-based estimates of aboveground carbon density (Mg C ha⁻¹). The blue line indicates the average estimated relationship for temperate and boreal forests (standard error = 4 Mg C ha⁻¹); the green line shows the average relationship for lowland to montane tropical forests (standard error = 20 Mg C ha⁻¹). These regressions are derived from Lefsky *et al* (2002a) and Asner *et al* (2009a). The red line shows an example adjustment made to the tropical forest relationship (green line) using 10 randomly selected plots from a new forest location. This illustrates the ability to rapidly adjust LiDAR metrics for a new region using a modest number of field plots.

3.3. Conversion of LiDAR measurements to aboveground carbon density

Following the airborne LiDAR sampling of the stratified forest map (figure 4), the mapped canopy 3D structural information derived from LiDAR can be used to estimate aboveground carbon density (ACD; units of Mg carbon ha⁻¹). This step requires a set of 'LiDAR metrics'. Ground-based allometric equations have been used for years to estimate ACD from field measurements of tree diameters, height and wood density (Brown and Lugo 1984, Chave *et al* 2005). In contrast, LiDAR metrics are new, relating airborne measurements of forest 3D structure, including height and the vertical canopy profile, to field-based estimates of ACD. Whereas the basic LiDAR data are typically collected at a spatial resolution of about 1 m, LiDAR metrics are usually averaged at the plot level then regressed against plot-level ACD estimates (e.g. 0.1–1.0 ha). This approach parallels traditional field studies that use manual measurements of the diameter and height of each tree to estimate plot-level biomass.

There are multiple ways to relate LiDAR measurements to aboveground carbon density. Lefsky *et al* (2002a) derived LiDAR metrics for three temperate and boreal forest biomes, yielding a general equation:

$$\text{ACD (Mg C ha}^{-1}) = 0.378 \times \text{MCH}^2$$
$$r^2 = 0.84, \qquad p < 0.001 \tag{1}$$

where MCH is the mean vertical canopy profile height derived from the airborne LiDAR (figure 5). This is just one of several canopy vertical profile metrics developed from LiDAR, shown here simply as an illustration. For a detailed presentation of this and other metrics, see Lefsky *et al* (2002a, 2002b).

Developing generic LiDAR metrics for tropical forests has been more challenging. Although equations were developed by Drake *et al* (2003) for moist and wet tropical forests, they employed a LiDAR technology unique to NASA's research program; that is, they used technology that is not widely used in the commercial sector. Commercial LiDAR will be needed to support carbon mapping for REDD. To address this gap, Asner *et al* (2009a) derived equations relating airborne, commercial-grade LiDAR metrics to carbon densities for lowland to montane tropical forest:

$$\text{ACD (Mg C ha}^{-1}) = 0.844 \times \text{MCH}^2$$
$$r^2 = 0.80, \qquad p < 0.01. \tag{2}$$

Although equations (1) and (2) are shown as comparable examples, it is notable that equation (2) scales carbon densities from LiDAR measurements at a rate that is 2.2 times greater than for temperate and boreal forests from Lefsky *et al* (2002a). This is caused by forest-dependent differences in the wood density, stem diameter and the number of trees per unit area (e.g. boreal conifer versus lowland tropical). As a result, field plots are needed to adjust the slope of the relationship between MCH^2 and aboveground carbon density for different forest types. Field plots can be set up anywhere within the LiDAR coverage area, but should span a range of apparent biomass levels, from low to high. A relatively small number of plots spanning the biomass levels found within each forest type (e.g., fewer than 10) can increase the accuracy of the LiDAR-to-biomass conversion equations by up to 40% (figure 5). This issue remains an intense focus of research, but it is becoming clear that the traditional notion that hundreds of plots are required per vegetation type is not supported by the current LiDAR literature, thereby decreasing the need for very large forest inventory measurement programs. The LiDAR becomes the regional sampling approach, whereas field plots help to calibrate the LiDAR to forest conditions. A major advantage of this approach is that LiDAR can map thousands of hectares of forest per day, whereas field plots cannot achieve the same geographic coverage.

Output from this LiDAR mapping step includes estimates of aboveground carbon density at 0.1–1.0 ha resolution, along with error values derived from uncertainty in the LiDAR-to-biomass conversion equations employed. An example 5000 ha map of forest aboveground carbon densities at 0.1 ha resolution is shown in figure 6 for a gradient of lowland to montane rain forest types on Hawaii Island. The resulting distribution of aboveground carbon densities is shown in the lower left panel. Current estimated uncertainties in the relationship between airborne LiDAR forest structure and ACD range from about 10–15% for temperate and boreal forests (Lefsky *et al* 2002a, Popescu *et al* 2004 and many others) to 8–25% in tropical forests (Drake *et al* 2003, Asner *et al* 2009a). It is important to note that these uncertainties are similar to the error ranges reported for plot-based estimates of ACD. For example, Brown and Lugo (1984) estimate a 20% uncertainty in stand-level biomass estimates derived from forest volumes; Chave *et al* (2005) estimate standard errors in stand biomass of 12–20%; and Keller *et al* (2001) reported up to 50% uncertainty in a very detailed, large-area biomass study in the central

Brazilian Amazon. In short, the LiDAR-to-biomass estimation approaches can be as certain as the measurement-to-biomass (allometric) approaches used at the plot level.

3.4. Integration of LiDAR and satellite data

Following LiDAR survey, the statistical distribution of the sampled carbon densities can be applied to a satellite image to derive a map of aboveground carbon stocks, along with uncertainty bounds. A simulated regional image of forest carbon stock is shown in figure 7. The map depicts the regional distribution of forest cover, deforested lands and forest disturbed through selective logging. There are also areas of secondary forest regrowth. The distributions of carbon density are shown in the bottom panels, and color-coded to match the detailed forest stratification.

The baseline aboveground carbon map simulated in figure 7 covers an area of 8000 km^2 in the Brazilian Amazon. The amount of airborne LiDAR mapping required to apply distributions of carbon stocks to the satellite image depends upon the relative proportions of each forest stratum, the intensity and diversity of land-use activities within each forest stratum, and the relative emphasis placed on these areas for carbon accounting. The original forest type and forest cover stratification process illustrated in figures 2–4 determines the partitioning of LiDAR coverage. Within a forest stratum, LiDAR coverage requirements are dictated by the need to achieve a robust statistical distribution of estimated carbon densities. In the central Amazon, Keller *et al* (2001) showed that 1.3% of a *terra firme* forest required surveying to achieve a statistical representation of a 392 ha area. Estimates from a 5000 ha tropical rain forest suggest that less than a 1% LiDAR sampling of each forest stratum (e.g. lowland intact forest, bog forest, montane forest, etc) yields carbon density distributions that are statistically similar to those of each forest type (derived from Asner *et al* 2009a).

Following aboveground carbon mapping, it is possible to estimate belowground carbon densities, as well as carbon densities for coarse woody debris and other surface organic litter. The IPCC (2006) provides scaling factors which can be applied to the image of aboveground carbon densities. For example, belowground carbon is estimated at 0.37 times the aboveground carbon density for tropical rain forest (Mokany *et al* 2006), providing support for Tier II level analysis. The modest number of field plots deployed in the LiDAR calibration step described above can also be used to improve estimates of belowground and surface litter carbon densities (IPCC 2006), if time and funding permit, to aim for Tier III type accuracies.

4. Monitoring losses and gains in forest carbon

Following a baseline carbon mapping assessment, two ongoing measurement efforts are required to track carbon losses and gains into the future. Carbon losses can be monitored through the use of satellite technology. Forest clearing and degradation can be mapped at high resolution on an annual basis, or more often depending upon needs and availability of satellite
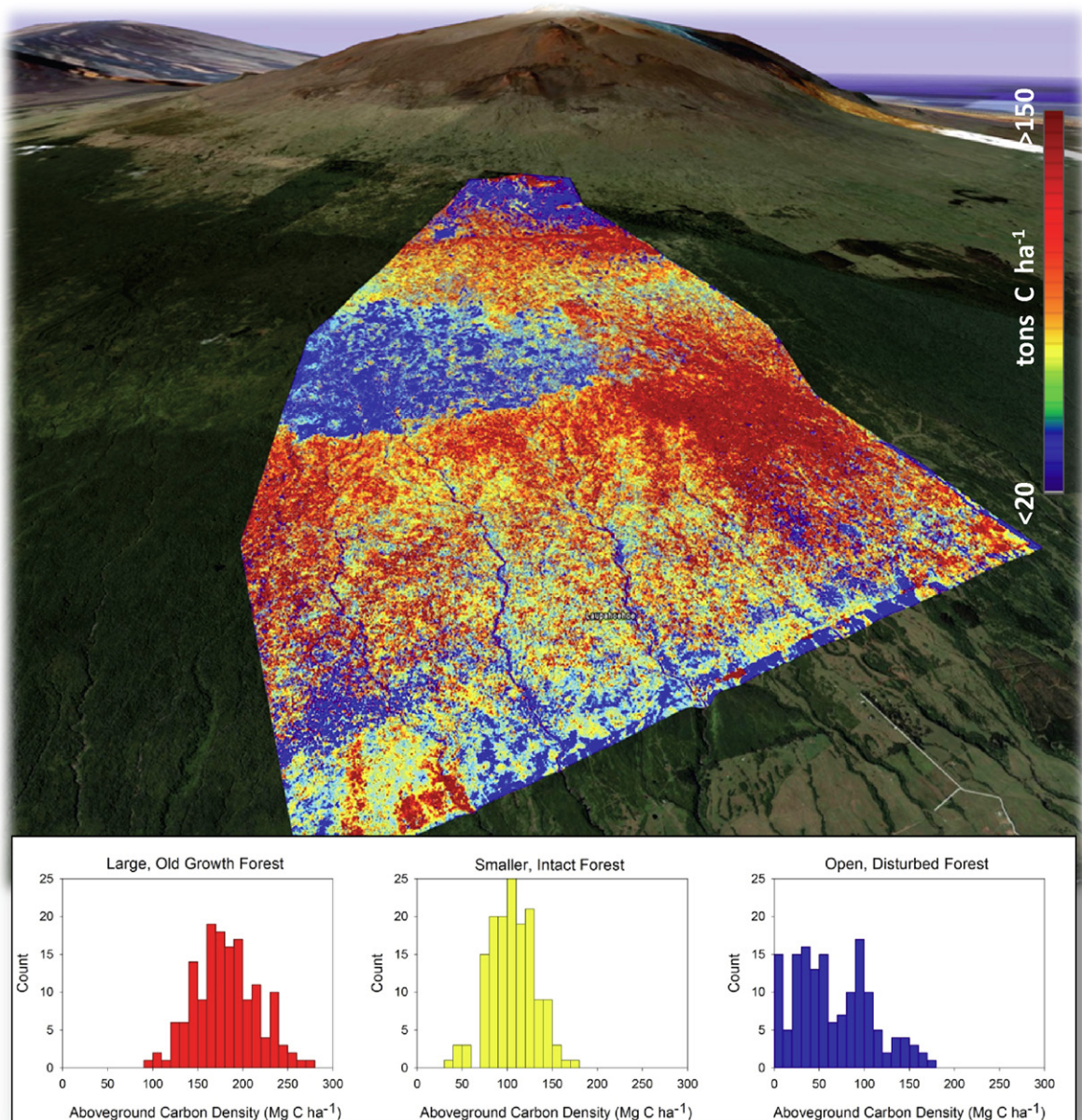
Figure 6. Aboveground biomass map (Mg C ha^{-1}) at 0.1 ha resolution derived from airborne LiDAR. This 4000 ha image was collected along the eastern slopes of Mauna Kea Volcano, Hawaii Island. The estimated distribution of aboveground biomass in large/old growth, smaller/intact, and open/disturbed rain forests are shown in the lower left panel.

imagery (DeFries *et al* 2005, GOFC-GOLD 2009). For example, deforestation and degradation maps derived from CLASlite can be applied to the baseline carbon stock map to estimate carbon emissions to the atmosphere (figure 8). Pitfalls here include uncertainty in converting satellite measurements of forest degradation to carbon loss, although the IPCC (2006) provides guidelines on ways to do this accounting.

A conservative, quantitative approach to monitoring carbon emissions following a baseline assessment is to multiply the fractional canopy loss within each CLASlite pixel by the carbon density value derived from the baseline carbon map. For example, a pixel might transition from 100% forest cover (CLASlite baseline) with 50 Mg C/pixel (LiDAR baseline) to 50% forest cover following selective logging,

resulting in an estimated 25 Mg C emitted to the atmosphere. Accuracy can be increased via rapid field assessment of actual carbon losses.

Long-term assessment of carbon gains requires that the region be continuously monitored for the onset of secondary regrowth following clearing; multi-temporal satellite imaging can greatly enhance this capability. A second requirement is to estimate the accumulation of carbon stock on a per-pixel basis. Many models and equations are available to support this approach, and these models may take into consideration forest and soil type as well as climate (Angelson *et al* 2009). The IPCC (2006) provides guidelines for incrementing carbon pools. The production of stored wood, surface woody debris and other litter can be tracked using either simple book-
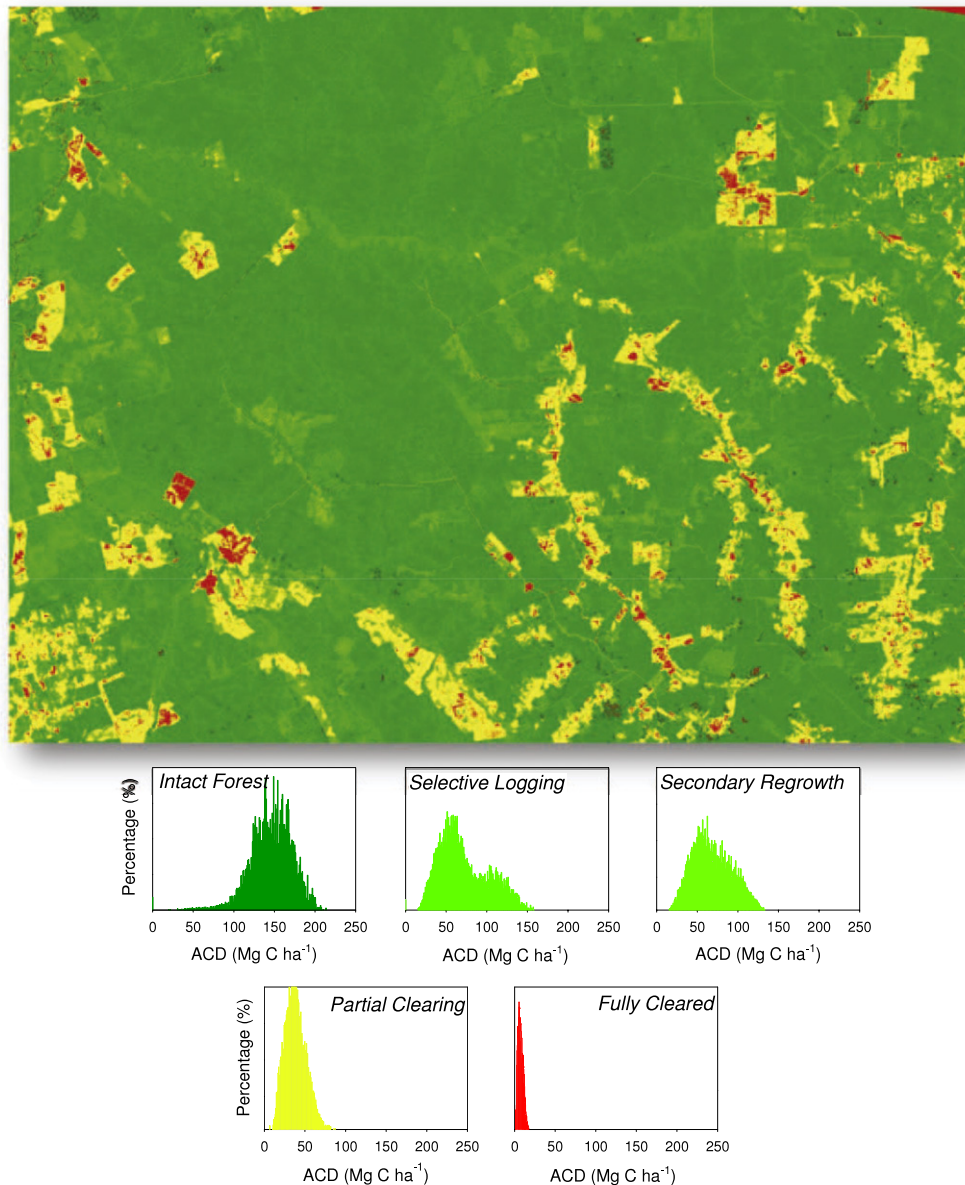
Figure 7. Simulated carbon landscape derived from CLASlite imagery taken over an 8000 km^2 region of the eastern Brazilian Amazon. Histograms simulate distributions of aboveground carbon density for each land cover stratum, applied for this demonstration using airborne LiDAR data collected in Hawaii.

keeping approaches (e.g. Houghton *et al* 2000), or detailed process-oriented models (e.g. Huang *et al* 2008). Independent of the modeling approach, a program of continuous satellite monitoring of clearing, logging or other disturbances, as well as recovery, should be considered a core activity, with modeling and field verification ongoing. A modest investment in satellite monitoring effectively decreases the requirement for labor-intensive field inventories, and it decreases reliance on forest growth models.

5. Costs

The cost to implement this proposed method for high-resolution baseline assessment is rapidly decreasing. Satellite data are decreasing in cost, and the major data sources are now free of charge to end users. Although satellites are expensive to develop, deploy and maintain, the governments doing so are making the data available on the World Wide Web. Landsat 5 and 7 and the Chinese–Brazil CBERS-1 and 2 are good examples. The next generation Landsat, called the Landsat Data Continuity Mission (LDCM; http://landsat.usgs.gov), is being built now and will launch in 2012, and the next line CBERS sensors are in development (http://www.cbers.inpe.br). Other commercial operators such as SPOT Image Corporation are making their data increasingly available, although not free of charge, and they have mature plans for new SPOT-6 and 7 satellites (http://www.spot.com). Several other sensors are also available (GOFC-GOLD 2009).
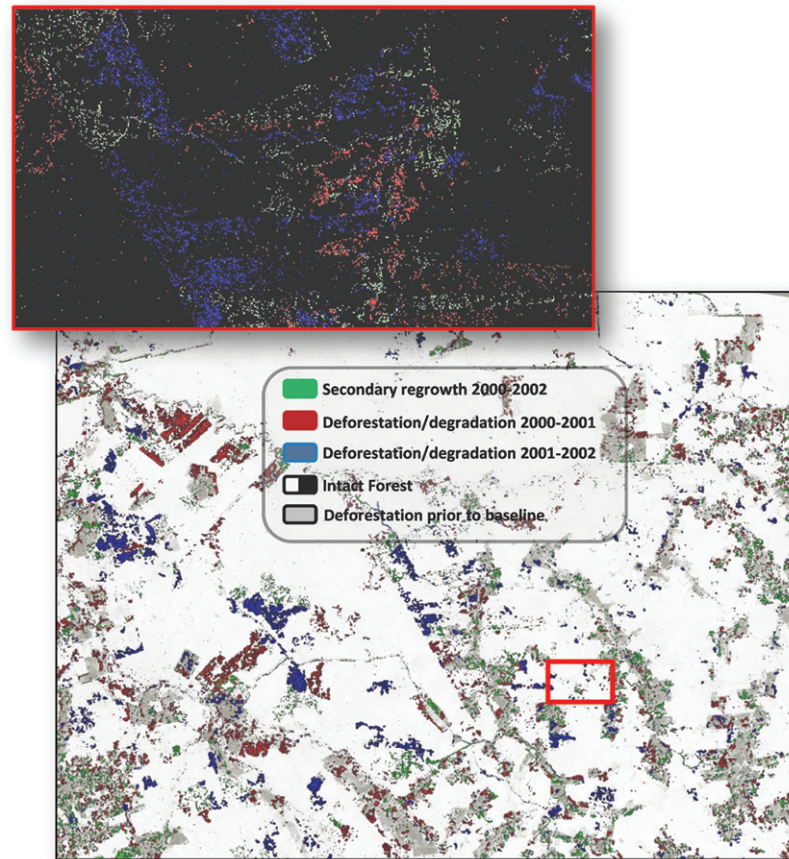
Figure 8. Long-term monitoring using annual CLASlite mapping of deforestation and degradation from 1999 to 2002 for a 8000 km^2 region in the eastern Brazilian Amazon. A zoom image (upper left, black) shows detail of forest degradation color-coded similarly to that of the deforestation map, revealing small-scale, sub-pixel forest canopy loss from selective logging. These maps can be used to estimate carbon emissions from the baseline map in figure 7.

The cost to analyze the satellite data for forest cover, deforestation and degradation is also rapidly diminishing. The Carnegie Institution is making CLASlite available for free to governments and NGOs throughout the Amazon region (http://landsat.gsfc.nasa.gov/news/news-archive/news_0182.html). The Brazilian Space Research Institute (INPE; http://www.inpe.br) and the Brazilian organization IMAZON (http://imazon.org.br) are making their forest cover analysis software available as well. There is a small cost of initial training, and the need for an internet connection, but the methods are now highly automated and thus can be operated by an entry-level technician.

LiDAR is a powerful airborne imaging technology that, like aerial photography in the 1970s–1980s, is rapidly expanding throughout the world for use across a range of environmental sectors. Airborne LiDAR is now widely used for mapping infrastructure including power lines, dams, and cities as well as terrain and forestry. As such, the commercial base is very strong, and it is supporting both an explosion of LiDAR technologies into many countries (and all continents) and a teaching of the next generation of remote sensing specialists. Such deep commercial support is unusual in remote sensing, and it speaks for the efficacy of the technology. There are now many airborne LiDAR mapping companies spread across the Americas, Europe, Africa, Asia, Australia and the Pacific (http://www.airbornelasermapping.com).

Today, the Carnegie Airborne Observatory can operate its LiDAR, process the data, and provide maps of forest structure at a cost of less than $0.20 per hectare, not including the cost of ferrying the aircraft and sensors to the theater of operation. This suggests that government or commercial LiDAR groups can operate within their own countries at similar or lower-cost levels. These costs are yet decreasing further with a new generation of fully automated LiDAR processing methods (http://www.ncalm.org). The methods could be disseminated in a manner parallel to that of the automated satellite mapping approaches that are supporting REDD baseline assessments and monitoring. I believe these advances in automation will decrease the dependence on specialists, just as we have seen with satellite deforestation mapping, resulting in LiDAR mapping costs of as little as $0.05 per hectare. Even beyond airborne LiDAR, new government-supported spaceborne LiDAR technology intended to measure forest structure worldwide may become available in late 2015 (http://desdyni.jpl.nasa.gov). Spaceborne LiDAR will provide the much added benefit of allowing continual reassessment of carbon densities in a spatially explicit and contiguous manner.

G P Asner

The costs of well-maintained field inventory plots remains highly variable, but likely not any lower than that of LiDAR. Take into account the fact that airborne LiDAR can cover far more forest in a day (>5000 ha) than can ever be measured on the ground by the same number of personnel, combined with the fact that field inventory methods of aboveground biomass appear no more accurate than LiDAR-based approaches (discussed earlier), and it seems that the methods are becoming interchangeable or at least highly compatible. Field plots are still needed to calibrate and validate LiDAR measurements to biomass, but the number of plots is greatly reduced since there is less need to sample the forest with plots, but rather focus the plots on calibrating the LiDAR. The LiDAR then becomes the forest sampling (or mapping) step in place of the plots.

Forest carbon monitoring at IPCC Tiers II/III is currently considered technically challenging, potentially labor-intensive and thus an expensive undertaking. Here I have proposed that a combination of free satellite monitoring technology with infrequent aircraft-based mapping can provide baseline carbon estimates and can improve the monitoring of carbon stocks, losses and recovery in forests. These tools are available now, and can be implemented in any region of the world, making rapid Tier II/III mapping a reality.

Acknowledgments

References

Achard F, Defries R, Eva H, Hansen M, Mayaux P and Stibig H-J 2007 Pan-tropical monitoring of deforestation *Environ. Res. Lett.* **2** 045022

Angelson A, Brown S, Loisel C, Peskett L, Streck C and Zarin D 2009 *Reducing Emissions from Deforestation and Forest Degradation (REDD): An Options Assessment Report* Prepared for the Government of Norway by the Meridian Institute, March 2009. Available for download at http://www.REDD-OAR.org; ISBN: 978-0-615-28518-4

Asner G P, Broadbent E N, Oliveira P J C, Keller M, Knapp D E and Silva J N M 2006 Condition and fate of logged forests in the Brazilian Amazon *Proc. Natl Acad. Sci. USA* **103** 12947–50

Asner G P, Hughes R F, Varga T A, Knapp D E and Kennedy-Bowdoin T 2009a Environmental and biotic controls over aboveground biomass throughout a rainforest *Ecosystems* **12** 261–78

Asner G P, Keller M, Pereira R, Zweede J C and Silva J N M 2004 Canopy damage and recovery after selective logging in Amazonia: field and satellite studies *Ecol. Appl.* **14** S280–98

Asner G P, Knapp D E, Balaji A and Paez-Acosta G 2009b Automated mapping of tropical deforestation and degradation: CLASlite *J. Appl. Remote Sens.* **3** 033543

Asner G P, Knapp D E, Broadbent E N, Oliveira P J C, Keller M and Silva J N M 2005 Selective logging in the Brazilian Amazon *Science* **310** 480–2

Asner G P, Knapp D E, Jones M O, Kennedy-Bowdoin T, Martin R E, Boardman J and Field C B 2007 Carnegie airborne observatory: in-flight fusion of hyperspectral imaging and waveform light detection and ranging for three-dimensional studies of ecosystems *J. Appl. Remote Sens.* **1** 013536

Brown I F, Martinelli L A, Thomas W W, Moreira M Z, Ferreira C A and Victoria R A 1995 Uncertainty in the biomass of Amazonian forests: an example from Rondonia, Brazil *Forest Ecol. Manag.* **75** 175–89

Brown S and Lugo A E 1984 Biomass of tropical forests: a new estimate based on forest volumes *Science* **223** 1290–3

Brown S, Pearson T, Slaymaker D, Ambagis S, Moore N, Novelo D and Sabido W 2005 Creating a virtual tropical forest from three-dimensional aerial imagery to estimate carbon stocks *Ecol. Appl.* **15** 1083–95

Cairns M A, Brown S, Helmer E H and Baumgardner G A 1997 Root biomass allocation in the world's upland forests *Oecologia* **111** 1–11

Chambers J Q, Asner G P, Morton D C, Anderson L O, Saatchi S S, Espirito-Santo D B, Palace M and Souza C Jr 2007 Regional ecosystem structure and function: ecological insights from remote sensing of tropical forests *Trends Ecol. Evol.* **22** 414–23

Chave J *et al* 2005 Tree allometry and improved estimation of carbon stocks and balance in tropical forests *Oecologia* **145** 87–99

DeFries R, Asner G P, Achard F, Justice C, Laporte N, Price K, Small C and Townshend J 2005 Monitoring tropical deforestation for emerging carbon markets *Tropical Deforestation and Climate Change* ed P Moutinho and S Schwartzman (Belém: Amazon Institute for Environmental Research)

Drake J B, Knox R G, Dubayah R O, Clark D B, Condit R, Blair J B and Hofton M 2003 Above-ground biomass estimation in closed canopy neotropical forests using lidar remote sensing: factors affecting the generality of relationships *Glob. Ecol. Biogeogr.* **12** 147–59

Gibbs H K, Brown S, Niles J O and Foley J A 2007 Monitoring and estimating tropical forest carbon stocks: making REDD a reality *Environ. Res. Lett.* **2** 045023

GOFC-GOLD 2009 Reducing greenhouse gas emissions from deforestation and degradation in developing countries: a sourcebook of methods and procedures for monitoring, measuring and reporting *GOFC-GOLD Report, Version COP14-2* GOFC-GOLD Project Office, Natural Resources Canada, Alberta, Canada

Hirsch A I, Little W S, Houghton R A, Scott N A and White J D 2004 The net carbon flux due to deforestation and forest re-growth in the Brazilian Amazon: analysis using a process-based model *Glob. Change Biol.* **10** 908–24

Houghton R A, Skole D L, Nobre C A, Hackler J L, Lawrence K T and Chomentowski W H 2000 Annual fluxes of carbon from deforestation and regrowth in the Brazilian Amazon *Science* **403** 301–4

Huang M, Asner G P, Keller M and Berry J A 2008 An ecosystem model for tropical forest disturbance and selective logging *J. Geophys. Res.* **113** G01002

IBGE 1993 *Mapa de Vegetacao do Brasil (Vegetation Map of Brazil)* 2nd edn, Instituto Brasiliero de Geografia e Estatistica (Brazilian Institute of Geography and Statistics)

IPCC 2006 *IPCC Guidelines for National Greenhouse Gas Inventories* ed H S Eggleston, L Buendia, K Miwa, T Ngara and K Tanabe, Prepared by the National Greenhouse Gas Inventories Programme, IGES, Japan

Keller M, Asner G P, Silva N and Palace M 2004 Sustainability of selective logging of upland forests in the Brazilian Amazon: carbon budgets and remote sensing as tools for evaluating logging effects *Working Forests in the Neotropics: Conservation Through Sustainable Management?* ed D J Zarin, J R R Alavalapati, F E Putz and M Schmink (New York: Columbia University Press) pp 41–63

Keller M, Palace M and Hurtt G 2001 Biomass estimation in the Tapajos National Forest, Brazil: examination of sampling and allometric uncertainties *Forest Ecol. Manag.* **154** 371–82

Lefsky M A, Cohen W B, Harding D J, Parker G G, Acker S A and Gower S T 2002a LiDAR remote sensing of above-ground biomass in three biomes *Glob. Ecol. Biogeogr.* **11** 393–9

Lefsky M A, Cohen W B, Parker G G and Harding D J 2002b LiDAR remote sensing for ecosystem studies *BioScience* **52** 19–30

Mokany K, Raison J R and Prokushkin A S 2006 Critical analysis of root:shoot ratios in terrestrial biomes *Glob. Change Biol.* **12** 84–96

Olander L P, Gibbs H K, Steininger M K, Swensen J J and Murray B C 2008 Reference scenarios for deforestation and forest degradation in support of REDD: a review of data and methods *Environ. Res. Lett.* **3** 025011

Phillips O L *et al* 1998 Changes in the carbon balance of tropical forests: evidence from long-term plots *Science* **282** 439–42

Popescu S C, Wynne R H and Scrivani J A 2004 Fusion of small-footprint lidar and multispectral data to estimate plot-level volume and biomass in deciduous and pine forests in Virginia, USA *Forest Sci.* **50** 551–65

Saatchi S S, Houghton R A, Dos Santos Alvala R C, Soares J V and Yu Y 2007 Distribution of aboveground live biomass in the Amazon basin *Glob. Change Biol.* **13** 816–37

Souza C, Roberts D A and Cochrane M A 2005 Combining spectral and spatial information to map canopy damages from selective logging and forest fires *Remote Sens. Environ.* **98** 329–43